Semiconductors, 2023, Vol. 57, No. 4

Switching (turn-on) dynamics of low-voltage InP homothyristors

© *S.O. Slipchenko, O.S. Soboleva, A.A. Podoskin, Y.K. Kirichenko, T.A. Bagaev, I.V. Yarotskaya, N.A. Pikhtin*

Ioffe Institute,
194021 St. Petersburg, Russia

E-mail: SergHPL@mail.ioffe.ru

Received April 13, 2023
Revised May 18, 2023
Accepted May 18, 2023

A series of heterostructure designs of low-voltage InP homothyristors have been investigated using numerical simulation methods. The design with a space charge layer formed in the p-base region of the $n-p-n$ transistor part was considered as the base one. The dynamic characteristics and processes that determine the rate of transition to the on state are investigated. It is shown that as the p-base thickness increases from 1 to 2.6 μm, the maximum on-state currents increase from 70 to 90 A, while the minimum turn-on transition time is 11 ns at a maximum blocking voltage of 55 V. It is shown that the operation efficiency in the on state is determined by the residual voltage. Residual voltage decreases with a decrease in the thickness of the p-base.

Keywords: thyristor, impact ionization, drift-diffusion model.

DOI: 10.61011/SC.2023.04.56428.4851

1. Introduction

The task of developing solid-state switches capable of switching high currents is relevant for the creation of powerful pulsed radiation sources based on semiconductor lasers [1–5]. Since semiconductor lasers have a low ohmic resistance, which can be tens mOhm, the voltage drop across a low impedance load does not exceed units V even when the required pulse amplitudes reach values of tens and hundreds A. In this case, there is no need to use high voltage switches. Another important criterion of solid-state keys for the considered range of tasks is the transient speed, which determines the possibility of forming pulses of the required duration. At present, the most interesting solutions are those that allow the formation of current pulses with a duration of units and tens ns, since the main application of pulsed lasers is related to distance measuring. In this case, the parasitic inductances of the current loop can significantly reduce the transient speed. For this reason, key designs must realize conditions for compact placement in a circuit with semiconductor lasers. In general, two approaches can be distinguished: (1) is based on switches closing the current circuit with the stored energy source in the form of a capacitor (transistor or thyristor-type current switches) [1–5], (2) is based on devices opening the current circuit with the stored energy source in the form of an inductive element [6]. Field-effect transistors are currently the most widely used. In first of all, it is connected with availability due to wide spread for solving problems in power and microwave radioelectronics. They allow to create conditions for pumping semiconductor lasers with current pulses of amplitude up to hundreds A and duration up to 10 ns [5], for effective operation of such systems additional specialized fast drivers are required, which provide conditions for fast switching on and off of high-current field-effect transistors. Despite this, compact realization of such circuits with a total area of a few cm IFx2x is possible. In [3,7], an approach based on hybrid integration of a GaAs–heterothyristor-based low-voltage key is proposed, where the ability to generate pulse durations in the range of 3–60 ns and current amplitudes up to 100 A is demonstrated. The advantage of this approach is the possibility of hybrid integration of semiconductor laser crystals and thyristor key, which ensures the smallest possible dimensions. The absence of high requirements for control pulses of low-voltage thyristors allows to simplify and reduce the size of the external control circuit.

In the present paper, the feasibility of low-voltage homo-thyristors based on InP has been investigated by numerical modelling techniques. This material is not inferior to GaAs in the main characteristics: mobility of charge carriers, breakdown voltage. In this case, the homo-thyristor design is the most technologically advanced, as it does not require the use of complex multi-component solid solutions. It is important to note that studies of low-voltage fast homo-thyristors based on $A^{III}B^{V}$ semiconductors have not been carried out previously. Besides, the developed solutions can be further developed in the direction of creation of integrated laser-thyristor keys based on InGaAsP/InP heterostructures allowing to obtain radiation in the spectral range 1300–1900 nm.

2. InP-based homo-thyristor model

Previous studies of AlGaAs/GaAs hetero-styristors have shown that the on-state transition rate has a significant effect on the dynamics of the generated current pulses [8,9]. For this reason, within the framework of this paper for low-voltage InP homo-thyristors, the dynamics of switching on is investigated and the issues of transition to the switched-off state are not investigated, as well as the influence of homo-thyristor design parameters on the speed of transients is analyzed. The overall structure of the InP homo-thyristor included a heavily doped n-InP emitter ($N_d = 10^{18}\,\text{cm}^{-3}$) with a thickness of $1\,\mu$m, a generally composite p- base based on a heavily doped thin p^+ InP layer ($N_a = 10^{18}\,\text{cm}^{-3}$) with a thickness of 0. $05\,\mu$m and a lightly doped part of p_0 InP ($N_a = 1.7 \cdot 10^{16}\,\text{cm}^{-3}$), a heavily doped n-InP ($N_d = 2 \cdot 10^{18}\,\text{cm}^{-3}$) collector $1.25\,\mu$m thick, for an $n-p-n$ transistor. The concentration level in the lightly doped part of the p-base was chosen based on the requirements of achievability and controllability for the metal-organic compound (MOC)-hydride epitaxy deposition process. The design of the p-base $n-p-n$ transistor, namely the thickness of the p_0-layer and the presence or absence of the p^+-layer were parameters to be optimized in the turn-on rate study. In turn, it is the design of the p-base that determines the blocking voltage of the homo-thyristor, and since the device to be developed must operate on a low impedance load, the maximum blocking voltages and hence the upper limit of the p-base thickness range were limited to 60 V and $2.6\,\mu$m, respectively. For the $p-n-p$ transistor, the p-emitter was formed by layer p-InP ($N_a = 3 \cdot 10^{18}\,\text{cm}^{-3}$) with a thickness of $0.25\,\mu$m.

The inclusion dynamics was calculated within the standard drift-diffusion model with impact ionization and negative differential mobility in the p_0 InP base layer, where the field domain of the reverse biased $p-n$ transition [8] was formed. Switching was performed by applying an electrical control pulse through the n-collector of the $n-p-n$ transistor, providing a current amplitude of 15 mA. The turn-on dynamics was calculated with an external $R-L$ circuit that included an equivalent resistance of 0.5 Ohm and an inductance of 1 nGn, the area of the calculated structures was $200 \times 500\,\mu\text{m}^2$, which is close to the values used in low-voltage current switches based on AlGaAs/GaAs [7] hetero-thyristors.

Shock ionization was described within the framework of the Selberherr model well established for the description of low-voltage AlGaAs/GaAs laser thyristors [8] and uses the following relationship between shock ionization coefficients and electric field strength [10]:

$$\alpha_{n,p}(E) = A_{n,p} \exp\big(-(B_{n,p}/E)^{\beta}\big), \qquad (1)$$

where the model parameters are $A_n = 2.93 \cdot 10^6$, $B_n = 2.64 \cdot 10^6$, $A_p = 1.62 \cdot 10^6$, $B_p = 2.11 \cdot 10^6$, $\beta = 1.0$. It is important to note here that a number of experimental results have demonstrated a lower impact ionization rate in InP compared to GaAs [11]. The authors attribute this to the larger value of the density of states in InP and the resulting higher electron-phonon scattering rate.

For a number of direct-gap semiconductors, such as GaAs and InP, when electrons move in strong electric fields with strengths greater than E_{pk}, there is a redistribution from Γ-valley, characterized by a lower effective mass, to L-valley, characterized by a higher effective mass. This transition leads to a decrease in the mean drift velocity, which in turn translates into a negative differential mobility. Since in the investigated devices the achieved electric field strengths can exceed E_{pk}, an analytical expression for the dependence of the electron mobility on the electric field strength was used to correctly describe the transport effects under such conditions. The analytical expression was proposed in [12] and obtained by approximating the experimental values of the electron drift velocity for the InP-based structures:

$$\mu_n = \frac{\mu_{n0} + \frac{\upsilon_{ns}}{E}\left(\frac{E}{E_t}\right)^{\gamma}}{1 + \left(\frac{E}{E_t}\right)^{\gamma}}, \qquad (2)$$

where E — electric field strength, E_t — electric field strength corresponding to the threshold of negative differential mobility (field at maximum drift velocity), μ_{n0} — mobility in weak electric fields, υ_{ns} — saturated electron drift velocity ($\upsilon_{ns} = 10^7$ cm/s), γ — model parameter ($\gamma = 2.3$). The model parameters are taken from [12]. The mobility of the holes was set in the usual way:

$$\mu_p = \frac{\mu_{p0}}{\big(1 + (E\mu_{p0}/\upsilon_{ps})^{\beta_p}\big)^{1/\beta_p}}, \qquad (3)$$

where μ_{p0} — mobility in weak electric fields, υ_{ps} — saturated electron drift velocity ($\upsilon_{ps} = 9 \cdot 10^6$ cm/s).

3. Simulation results and their analysis

Numerical modelling of the turn-on dynamics was performed for a series of InP homo-thyristor structures that differed in the p-base $n-p-n$ transistor design. Five p-base structures were considered: *1* — included only the p_0 InP layer with a thickness of $2.6\,\mu$m, *2* — included layers of p^+ and p_0 InP with thicknesses of 0.05 and $2\,\mu$m, respectively, *3* — included layers p^+ and p_0 InP with thicknesses of 0.05 and $1.5\,\mu$m, respectively, *4* — included layers p^+ and p_0 InP with thicknesses of 0.05 and $1\,\mu$m, respectively. The use of an p^+-layer placed on the n-emitter side avoids bridging of the bulk charge areas of the collector and emitter $p-n$ transitions and thus increases the operating range of the blocked voltages. Hereinafter, the specified types of base construction will be referred to as including only layer p_0 and a combination of layer p^+/p_0. The nature of the dynamic dependences obtained during calculations for all types of structures is similar, so let us consider typical dependences on the example of the 1st type structure.The dynamics of current and voltage for the 1st type structure is shown in Fig. 1. It can be seen that the dependencies obtained can be characterized by the current (maximum current) in the on state, which is determined by the blocking voltage (maximum blocking voltage) and the residual voltage in the on state, and the speed of transition to the on state, which is defined as the time it takes to reduce the blocking voltage from level 90% to level 10% in the open state. It can be seen that the blocking voltage affects the turn-on dynamics and current amplitude. We consider the distributions of the electric field modulus, charge carriers, hole current and shock ionization

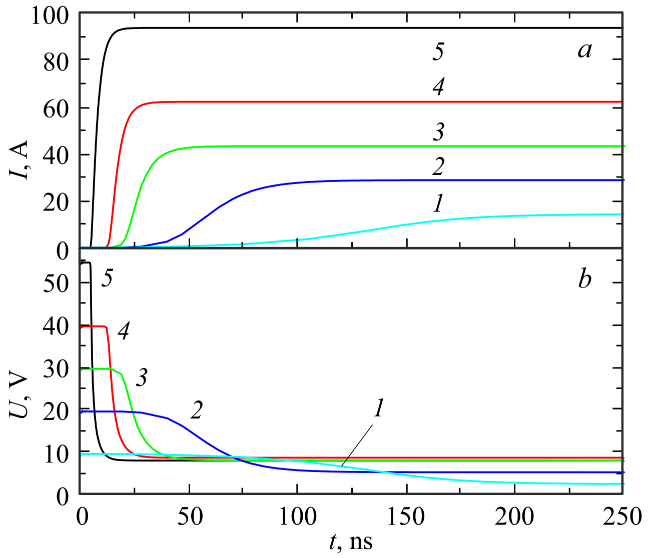

Figure 1. Current (a) and blocking voltage (b) dynamics dependence at switching on InP homo-thyristor with p-base construction based on the lightly doped layer with thickness of $2.6\,\mu$m and $p = 1.7 \cdot 10^{16}\,\text{cm}^{-3}$ alloying at various voltages, V: *1* — 10, *2* — 20, *3* — 30, *4* — 40, *5* — 55.

rate for the maximum blocking voltage at different time instants (Fig. 2). Five characteristic times were chosen for this purpose (Fig. 2, a): 0 — corresponds to the steady state at the set blocking voltage, 2.5 ns — corresponds to the state when the control current pulse is applied but the thyristor is still in the closed state, 5.9 ns — the time which corresponds to the beginning of the thyristor switching on, 10.3 ns — the time which corresponds to the end of the transient at the edge of the thyristor switching on, and 103 ns — the time when the thyristor is open.

If we consider the emitter $p{-}n$ transition $n{-}p{-}n$ transistor part, the field for the $\sim 0.25{-}0.5\,\mu$m area corresponds to the p-base layer. Since the emitter $p{-}n$ transition is formed by a highly doped n-layer ($N_d = 10^{18}\,\text{cm}^{-3}$) and a lightly doped p-layer ($N_a = 1.7 \cdot 10^{16}\,\text{cm}^{-3}$), the bulk charge area is mainly located in the p-base layer and formed by negatively charged acceptors. At time 0, when only the blocking voltage is applied, the field distribution in the emitter $p{-}n$ transition is close to stationary without applying an external voltage, since the leakage currents through the structure are negligibly small. For a time instant of 2.5 ns, the current density through this $p{-}n$ transition is also negligible ($< 10\,\text{A/cm}^2$), so the field distribution for the equilibrium state ($t = 0$) and 2.5 ns after the application of the control pulse differ only slightly. Significant field redistribution at the emitter $p{-}n$ transition begins when the thyristor opens, when the current through the device markedly increases.

Fig. 2, c shows that the transition to the switched-on state is accompanied by field redistribution in the area of the collector $p{-}n$ transition, which is expressed in

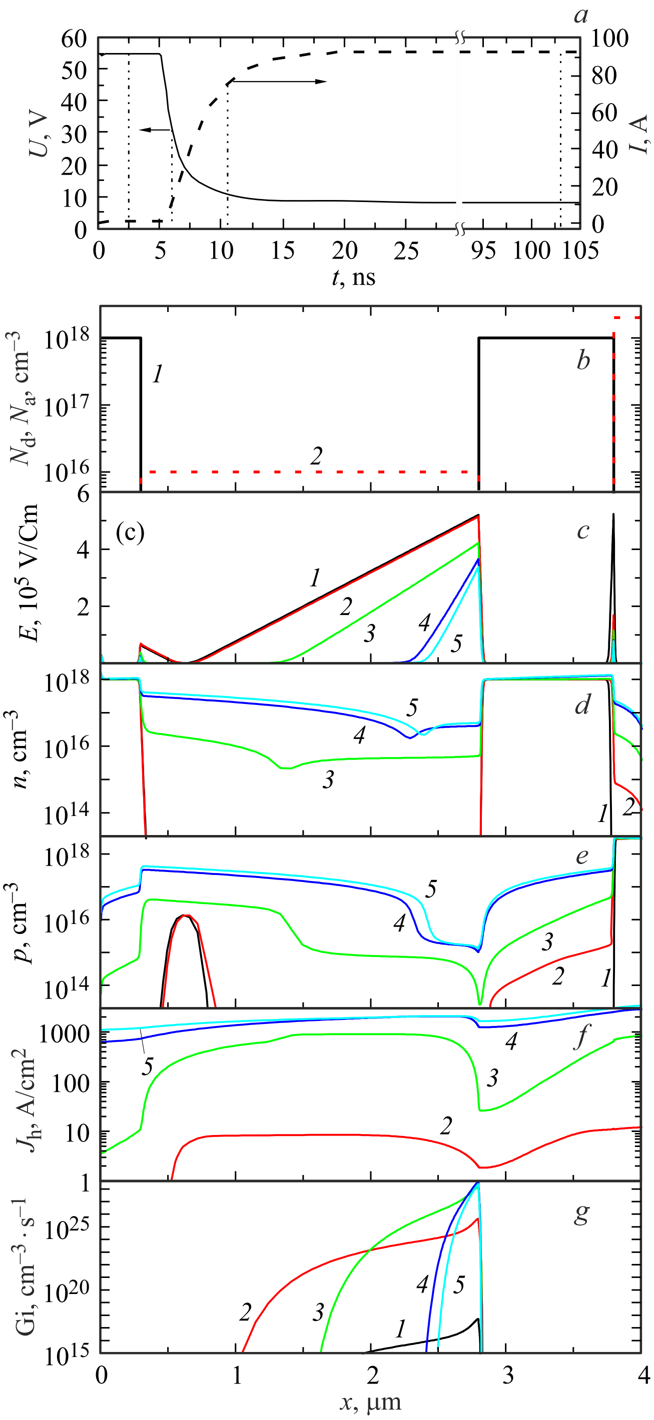

Figure 2. a — voltage and current dynamics during the transition of the homo-thyristor to the switched state at a blocking voltage of 55 V.The dotted lines show the time moments for which the distributions in the heterostructure layers of charge carrier concentrations, hole current density, electric field, and shock ionization rate are given. b — distribution of alloying impurities in the layers of the modelled homo-thyristor structure: *1* — donor, *2* — acceptor. Distributions in the layers of the homo-thyristor structure of the electric field modulus (c), electrons (d), holes (e), hole current density (f), shock ionization rate (g) for different time moments, ns: *1* — 0, *2* — 2.5, *3* — 5.9, *4* — 10.3, *5* — 103.

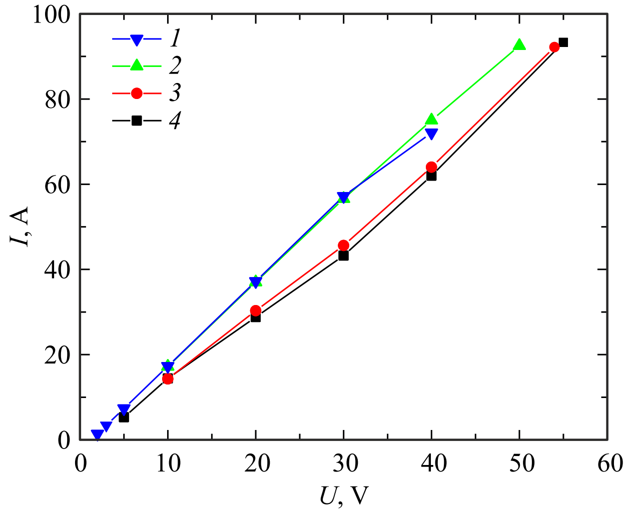

Figure 3. Voltage dependences of open-state current for InP-homo-thyristor designs with different thicknesses *p*-base, μm: *1* — 1, *2* — 1.5, *3* — 2, *4* — 2.6.

a narrowing of the field domain and a decrease in its amplitude. However, it is important to note that even in the open state, a narrow field domain with a sufficiently high amplitude reaching $3.3 \cdot 10^5$ V/cm is preserved in the area of the collector $p-n$ transition. Significant changes in the distributions of excess charge carriers are also observed: the transition to the on-state is accompanied by an increase in the concentration of both excess electrons and holes in the *p*-base area, with the concentration value of both types of carriers in the open state exceeding 10^{17} cm^{-3} (Fig. 2, *d, e*). Let us consider the main mechanisms determining the accumulation of excess holes in *p*-base. Fig. 2, *f* shows the hole current for selected time instants. It can be seen that the hole current component associated with the injection from the anode contact drops markedly in the area of the doped *n*-base at the initial stage of switching on, which is associated with non-radiative recombination in the *n*-layer. In result, the main source is shock generation in the reverse biased collector $p-n$ transition area of the $n-p-n$ transistor part. Fig. 2, *g* shows the distribution of the shock ionization rate at different time instants. It can be seen that, despite the maximum field strength at the time period 0–2.5 ns, the shock ionization rate is small because it is significantly limited by the low current through the $p-n$-transition. The onset of switching on is accompanied by a significant increase in the shock ionization rate, as can be seen from the dependence for time 5.9 ns (Fig. 2, *g*), despite the narrowing of the electric field domain and a drop in its amplitude (Fig. 2, *c*). Thus, for low-voltage homo-thyristors, the rate of transition to the on state at voltages close to the maximum blocking voltage is determined by the rate of impact ionization in the field domain area.

Fig. 3 shows the dependences of the open state current on the blocking voltage obtained for the investigated types of InP homo-thyristor designs. It can be seen that the maximum open state current reaches 90 A and is limited by the maximum blocking voltage reaching 55 V for structures with base thicknesses 2 μm (p^+/p_0 base design) and 2.6 μm (p_0 base design). It can be seen that by using the p^+/p_0 base design, its thickness can be reduced while maintaining a high blocking voltage. Exceeding the maximum blocking voltage is accompanied by an uncontrolled transition of the homo-thyristor to the open state. For a 4 type structure with a minimum base thickness 1 μm, the maximum blocking voltage does not exceed 40 V, as a consequence, the achievable value of the maximum current in the open state has the minimum value of 70 A among all the structures studied. Although the structures 1 and 2 types with base thicknesses of 2.6 and 2 μm, respectively, exhibit higher maximum blocking voltages, they are inferior in efficiency, i.e. these structures exhibit lower open-state current at the selected blocking voltage. To clearly demonstrate the open-state efficiency of the investigated types of InP homo-thyristor designs, we consider the dependences of the open-state residual voltage fraction expressed as a percentage of the blocking voltage (Fig. 4). It can be seen that it is the structures 1 and 2 type with thick *p*-base that exhibit higher residual stress. The large magnitude of the residual voltage is primarily due to the need to maintain the required field in the area of the field domain that persists even in the switched-on state (Fig. 2, *c*) in order to provide the required drift current. As a result, for the 1 and 2 type structures, when the blocking voltage is increased from 10 to 55 V, the residual voltage fraction decreases from 27 to 15%. The reason for the increase in the switching efficiency of the homo-thyristor when the blocking voltage is increased is due to the increase in the shock ionization rate in the electric field domain formed at the *p*-base/*n*-collector boundary, which provides a more efficient supply of excess

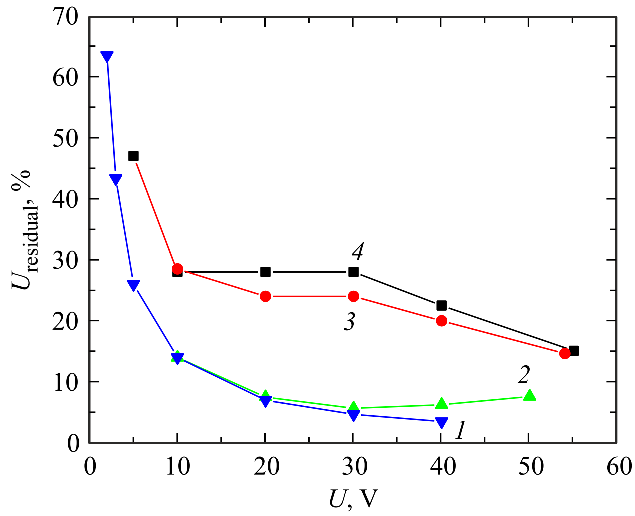

Figure 4. Dependences of the open-state residual voltage fraction, expressed as a percentage of the blocking voltage, for InP-homo-thyristor designs with different thicknesses *p*-base, μm: *1* — 1, *2* — 1.5, *3* — 2, *4* — 2.6.

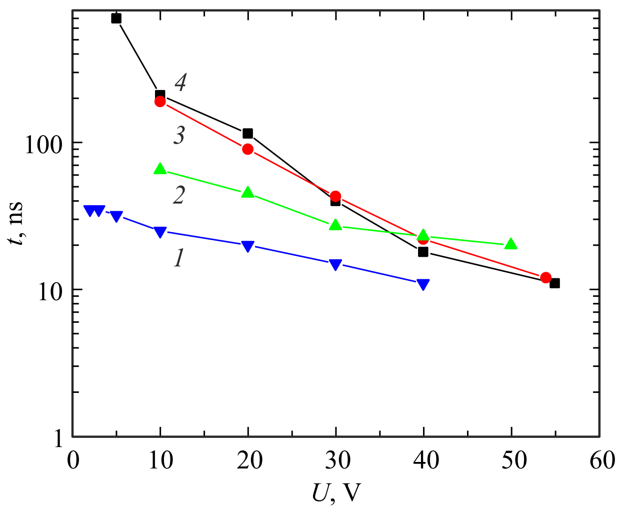

Figure 5. Voltage dependence of open state transition time for InP-homo-thyristor designs with different thicknesses p-base, μm: *1* — 1, *2* — 1.5, *3* — 2, *4* — 2.6.

holes to p-base. It is important to note that it is the excess holes for the p-base that provide the required current gain of the $n-p-n$ transistor. Clearly, the important role of impact ionization is noticeable in the transition to the low blocking stress area. Thus, in the 1 type structure at an operating voltage of 5 V, when impact ionization is practically inactive, the fraction of residual increases to 47%. Reducing the thickness of the p base also allows for more efficient operation when switched on. It can be seen that for type 3 and 4 structures, when the blocking voltage is increased from 10 to 50 V, the proportion of residual stress decreases from 13 to 7.5%. At the same time, there is still a sharp increase in the residual stress fraction in the area of smaller values of blocked voltages (< 10 V). As a result, the residual voltage can be up to 45% of the blocked voltage.

To solve the problem of generating short pump current pulses, one of the important parameters is the turn-on rate. The dependences of the switch-on time on the blocking voltage for the considered types of structures are shown in Fig. 5. It can be seen that the on-state transition time decreases as the blocked voltage increases, with the value of the minimum on-time reaching 11 ns for the maximum blocked voltages. Reducing the blocking voltage to 10 V leads to an increase in the on-state transition time to 194 ns for the structures of 1 and 2 types. Reducing the base thickness significantly reduces the turn-on time for equal operating voltages. In result, for a structure with a minimum base thickness of 1 μm at a blocking voltage of 10 V, the turn-on time is 25 ns.

4. Conclusion

The conducted studies have shown that the designs of the p-base $n-p-n$ transistor area of the low-voltage homo-thyristor structure have a significant influence on the performance characteristics. In general, we can speak of an improvement in such characteristics as on-state transition rate and on-state efficiency for structures with minimum layer thickness p_0 of the base, when operating at the same blocking voltages. However, decreasing the thickness of the p_0 base layer also leads to a decrease in the maximum blocking voltage and consequently the maximum open state current. This means that the choice of design should be based on the specific requirements of the tasks to be performed. If high amplitudes of pumping current are required to solve the set tasks, the optimization of designs should be aimed at finding solutions related to increasing the maximum blocking voltage, and it should be expected that the maximum performance will be realized precisely in the area of maximum voltages. If operating efficiency and high switching speed are important for the widest possible operating voltage range, the operating structure should be selected with a minimum layer thickness of p_0 base. It is important to note that all the proposed solutions related to reducing the thickness of the p_0 base effectively work when using p^+ „backing layer".

Funding

The authors are grateful to the Russian Science Foundation for financial support for this research (project No. 22-79-10159).

Conflict of interest

The authors declare that they have no conflict of interest.

References

[1] A. Klehr, A. Liero, H. Christopher, H. Wenzel, A. Maaßdorf, P. Della Casa, J. Fricke, A. Ginolas, A. Knigge. Semicond. Sci. Techn., **35** (6), 065016 (2020).

[2] A. Klehr, H.J. Wünsche, A. Liero, T. Prziwarka, G. Erbert, H. Wenzel, A. Knigge. Semicond. Sci. Techn., **32** (4), 045016 (2017).

[3] S.O. Slipchenko, A.A. Podoskin, O.S. Soboleva, V.S. Golovin, D.N. Romanovich, V.A. Kapitonov, A.S. Kazakova, K.V. Bakhvalov, N.A. Pikhtin, T.A. Bagaev, M.A. Ladugin, A.A. Padalista, A.A. Marmalyuk, V.A. Simakov. IEEE Trans. Electron Dev., **68** (6), 2855 (2021).

[4] S.O. Slipchenko, A.A. Podoskin, V.S. Golovin, M.G. Rastegaeva, N.V. Voronkova, N.A. Pikhtin, V.A. Simakov. IEEE Phot. Techn. Lett., **33** (1), 11 (2020).

[5] T.A. Bagaev, N.V. Gul'tikov, M.A. Ladugin, A.A. Marmalyuk, Yu.V. Kurnyavko, V.V. Krichevskii, A.A. Morozyuk, V.P. Konyaev, V.A. Simakov, S.O. Slipchenko, A.A. Podoskin, N.A. Pikhtin, A.E. Kazakova, D.N. Romanovich, V.A. Kryuchkov. Quant. Electron., **51** (10), 912 (2021).

[6] A.A. Podoskin, I.V. Shushkanov, V.V. Shamakhov, A. Rizaev, M. Kondratov, A.A. Klimov, S.V. Zazoulin, S.O. Slipchenko, N.A. Pikhtin. Quant. Electron., **53** (1), 1 (2023).

[7] S.O. Slipchenko, A.A. Podoskin, V.S. Golovin, D.N. Romanovich, V.V. Shamakhov, D.N. Nikolaev, I.S. Shashkin, N.A. Pikhtin, T.A. Bagaev, M.A. Ladugin, A.A. Marmalyuk, V.A. Simakov. Opt. Express, **27** (22), 31446 (2019).

[8] V.S. Yuferev, A.A. Podoskin, O.S. Soboleva, N.A. Pikhtin, I.S. Tarasov, S.O. Slipchenko. IEEE Trans. Electron Dev., **62** (12), 4091 (2015).

[9] O.S. Soboleva, V.S. Golovin, V.S. Yuferev, P.S. Gavrina, N.A. Pikhtin, S.O. Slipchenko, A.A. Podoskin. Semiconductors, **54**, 575 (2020).

[10] S. Selberherr. *Analysis and Simulation of Semiconductor Devices* (Wien-N. Y., Springer).

[11] K. Brennan, K. Hess. Solid-State Electron., **27** (4), 347 (1984).

[12] G. Wedel, T. Nardmanrr, M. Schröter. 2018 IEEE BiCMOS and Compound Semiconductor Integrated Circuits and Technology Symp. (BCICTS), **1** (October 15–17, 2018, San Diego, California, USA).

Translated by Y.Deineka